JPIChE 53(1) 2025: 65-75

PAKISTAN INSTITUTE OF CHEMICAL ENGINEERS Since 1969

Journal of the Pakistan Institute of Chemical Engineers

Journal homepage: www.piche.org.pk/journals

DOI: https://doi.org/10.54693/piche.05316

Check for updates

Effect of Dextrin Content in Alcohol-Based Zircon Coating for Sand Mold Applications

M.Z. Yousuf[1], M.U. Manzoor[1]*, A. Salman[1]

Submitted: 27/02/2025, Accepted: 22/07/2025, Published: 13/10/2025

Abstract

Three alcohol-based zircon coating compositions were developed using a variation of dextrin binder for high-temperature steel castings in silica sand molds. The average particle size of zircon sand used in formulating the coatings was measured as 40 microns. The coatings were characterized by using Fourier Transform Infrared Spectroscopy (FTIR), thermal stability testing, surface roughness and permeability measurement. The results demonstrated that increasing the dextrin content principally improved the mold and casting surface finish. There was a significant improvement in an average surface roughness reduction of the mold, and by 25% of the casting. The permeability number of the sand mold with coating was reduced by more than 20% of that of the sand mold without coating, which greatly influenced in enhancing the mold-metal interface protection and reducing the casting surface defects. The thermal stability of the coating was observed from 200°C to 1600°C and no cracks and delamination were observed. The findings highlight the potential of dextrin as an effective binder in zircon coatings, optimizing performance for steel casting applications.

Keywords: Dextrin Binder, Zircon Coating, Surface Roughness, Permeability, Mold-metal Interface, Steel Casting, FTIR Analysis

1. Introduction:

In steel casting, the pouring temperature is extremely high, ranging from 1550~1600℃, requiring foundry coatings that can withstand such high temperatures and resist the burnt-on sand. Refractory coatings are used on sand molds and cores to prevent sand from sticking to the casting, improve surface smoothness, and avoid excessive metal penetration into the sand molds during the casting process [1]. This coating fills gaps between the grains of sand and provides a smooth mold surface for the molten metal. These coatings enhance surface smoothness and eliminate defects and cleaner shakeouts like metal penetration, sand burn-in, veining and erosion. The coating also enhances the surface quality of the casting and reduces the fettling and shot/sandblast costs during the casting process [2]. In a research, Milanova et al. [3] concluded that integrating the foundry coating and tribological science can enhance coating erosion resistance, improve casting surface quality, and reduce cleaning and finishing costs in foundries globally. Bian et al. [4] worked on rheology and gas evolution features of self-curing water-based coating for sand mold casting and found that the coating thickness must be minimal to improve the casting production efficiency, while the thick coatings should be applied in a single layer to maintain surface quality. Waseem et al. [5] characterize the alcohol-based foundry coating containing ferric oxide and silica with an average particle size of 75 microns as the main constituents. The design of experiment was for optimum

[1]*Institute of Metallurgy & Materials Engineering, Faculty of Chemical & Materials Engineering, Quaid-e-Azam Campus, University of the Punjab, Lahore, Pakistan ,*
Corresponding author: Muhammad Umar Manzoor (umar.imme@pu.edu.pk)

and economical coating composition. After applying the coating to gray cast iron sand mold, the qualitative and quantitative analysis confirmed the defect-free surface finish, without affecting the chemical composition and microstructural features. Zhan et al. [6] worked on an anti-carburizing water-based refractory coating, containing zirconium and silicate powder, for low-carbon steel alloys in resin-bonded sand molds. They claimed that the coating with zirconium exhibits excellent permeability, anti-flow properties and crack resistance. The carburizing layer thickness of 1 mm and max carburizing rate of 23.6% are achieved with silicate-based coating, whereas the carburizing layer thickness is double and the carburizing rate is thrice for the zircon powder coating. A water-based coating developed by Kmita et al. [1] showed superior performance as compared to the commercially available coating, yielding reduced surface roughness on sand molds. However, longer drying times compared to alcohol-based coatings were noted, impacting foundry yield, although alcohol-based coatings were found compatible with all sand mold types. Coating thickness and control of coating drying time play an important role in the quality of steel casting. Muoio et al. [7] studied the effect of different variables like sand compaction, coating density, dipping time and gravity on the coating layer properties. They concluded that the relations between coating layer properties and coating variables are scattered and non-linear. The scattering of the coating process can be controlled by selecting the right molding and coating parameters. Xu et al. [8] developed an alcohol-based zircon spraying coating on the green sand mold for steel casting. The coating showed excellent crack resistance at high temperatures and good surface finishing on the casting. Jamrozowicz et al. [9] coated the sand mold with water and alcohol-based single- and double-layer commercial coatings and investigated the drying behavior of the coating with gravimetric and ultrasonic techniques. The results showed that the second layer took 20-30% longer time to dry than the first layer and also the drying time of alcohol-based coating is shorter than the water-based coating. Under the atmospheric conditions, the viscosity played its role in coating drying time. Leushin et al. [10] worked on alumino slag-based coating from aluminium melt as anti-penetration coating for sand mold of ferrous alloys. The coating was based on refractory oxides such as alumina and silica with water and organic liquids as a solvent. They claimed that the alumino slag coating was comparatively cheaper and showed satisfactory results. The systematic study of dextrin content variation in alcohol-based zircon mold coatings for steel casting applications, has not been extensively investigated to the best of the author's knowledge. Prior studies have primarily explored water-based coatings or alcohol-based coatings with different binders like sodium silicate, phenolic resins, or commercial formulations. This study uniquely varies dextrin content (14–21%) in alcohol-based zircon coatings and evaluates its direct impact on average surface roughness of the mold and casting, permeability of the coated molds and thermal stability and cracking behavior of the coated molds.

2. Experimental Work:

The particular silica sand for the alpha-set molding process and zircon sand for the mold coating process were used in the research work. The particle size distribution of silica and zircon sand was determined by sieve analysis as per AFS 1105-12-S [11]. The mechanical horizontal sieving method was used. A representative particle sample of 100 grams was taken for each sand. The refractory aggregate as zircon sand, dextrin binders, Phenyl Formaldehyde (PF) resin and additives were mixed to prepare the coating. During preparation, the coating was stirred at

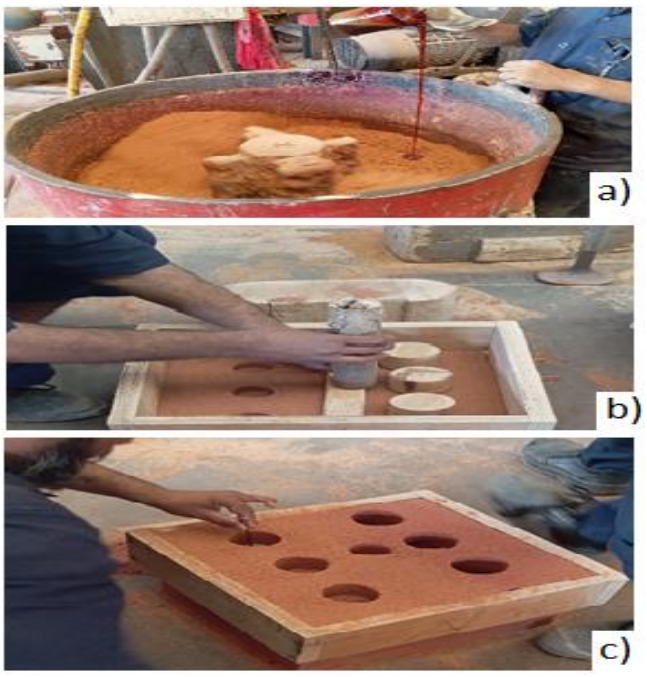

Figure 1: Alpha set sand mold/core preparation a) Mixing of sand with alpha set b) Making sprue and runner c) Cope and Drag

low speed to avoid precipitation, agglomeration and gas entrapment during agitation. Different percentage compositions of dextrin were taken as a binder. Three types of Alcohol-based Zircon coating samples (D15, D17, D20), as shown in table 1, were formulated with an average coating density of 1.5 g/cm^3.

Table 1: Different Samples Coating Composition

No.	Zircon (%)	Dextrin (%)	P. F. Resin (%)	Addit-ives %
D-15	60-65	14-16	0.5-1.5	0.5
D-17	60-65	16-18	0.5-1.5	0.5
D-20	60-65	19-21	0.5-1.5	0.5

FTIR analysis of coating formulations was conducted to confirm the presence of certain chemical compounds and the tests were carried out using Perkin-Elmer Spectrum 2 FTIR. The samples were scanned at the range of 4,000 cm^{-1} to 650 cm^{-1} with 15 numbers of scans. The loss of ignition test measures the weight loss of a sample when fired to a high temperature, which creates a similar effect as when molten metal is poured into the sand molds. The loss in weight is an indicator of weight loss due to gas generation, loss of chemically bound water and some weight gain due to oxidation when the test is not carried out in an inert atmosphere. The thermal stability of the coating was checked by igniting the samples with the flame to evaporate the excessive alcohol content on the surface followed by heating the coating to 120^{o}C for evaporation of compounds present within the sample. The samples were then heated to various temperatures and up to the pouring temperature of the furnace (200^{o}C, 400^{o}C, 600^{o}C, and 1200^{o}C) for thermal stability.

Alpha set sand molding process, also known as a self-setting sand system was used to prepare the sand molds. Table 2 shows the ratio of alpha set sand mold composition. A standard laboratory mixer was used for the mixing of sand and other ingredients.

Table 2: Constituent used in alpha sand mold

Resin (% wt. of Sand)	Hardener (% wt. of resin)	Curing time (min)
1.8	20	30

[12]

To assess the efficacy of three alcohol-based zircon coating formulations, four different types of Alfa set sand molds and cores (3 for coating compositions and 1 without coating) were prepared as shown in fig. 1. The sample marked as (D-N) is without coating, a controlled sample.

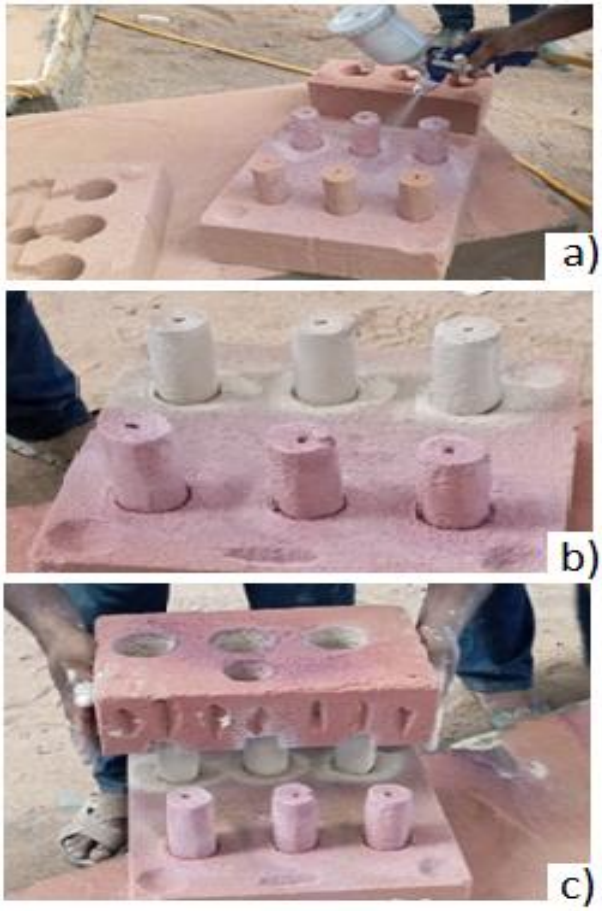

Figure 2: In a), b) and c) figures different formulations Alcohol-based zircon coating spraied with spay gun on sand mold/cores.

The hollow cylindrical shaped molds having an external diameter of 63.5 mm (2.5 inches) and the core with a diameter of 38.1 mm (1.5 inches) and 76.2 mm (3 inches) height were used to get a casted sample of 10 mm thickness. The roughness of the sand mold samples was measured with a portable surface roughness gauge profilometer (SRG-4600). The permeability number of a sand mold was measured using the formula as given in equation

$$Permeability\ Number\ (P) = \frac{VH}{APT} \quad (1)$$

where V is the air volume passing through the sand specimen, H is the sand specimen height (in cm), A is the sand specimen cross-sectional area (in cm^2), P is the pressure difference between two ends of the specimen (in cm of water) and T is the air passing time across the specimen (in minutes).

The formulated alcohol-based foundry coatings containing zircon sand were applied on the sand molds by spray gun as shown in fig. 2.

The spray gun used had a flow rate of 200 ml/min with an air pressure of 103 kPa. A thin coating was applied on to the surface of the mold. After the coating, the samples were dried off through flame ignition. The coating thickness was measured using a calibrated optical microscope from the cross-section of the mold. The roughness of the sand mold samples after coating was also measured. The permeability number of a sand mold with coating was measured as well.

In a foundry shop, an 8-ton induction furnace was utilized to make the alloy of medium carbon steel with the following composition as in Table 3.

Table 3: Chemical Composition of Medium Carbon Steel

Steel	AISI 1045
C	0.44
Si	0.15
Mn	0.86
Cr	0.017
Ni	0.0062
Mo	0.0007
S	0.008
P	0.016

When the metal temperature hit 1600^{o}C in the furnace, it was tilted to transfer the molten metal into the crucible. The molten metal from the crucible was then poured into the sand molds as shown in figure 3, and allowed to solidify. The molds are composed of a coating of zircon sand particles with different dextrin compositions and also a separate mold without coating.

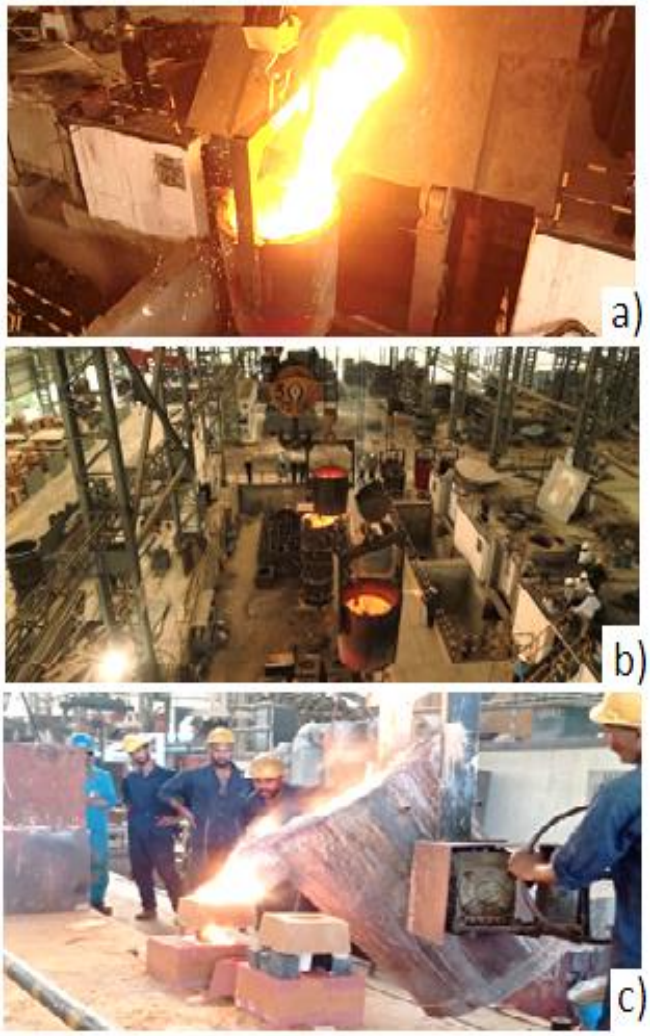

Figure 3: Melting of Steel for casting a) pouring of molten metal from furnace to crucible b) transferring of molten metal c) pouring of molten metal to molds

The solidification time for each sample was calculated using the Chvorinov's Rule formula shown in equation 2.

$$T = C_m \left(\frac{V}{A}\right)^2 \qquad (2)$$

where T represents the solidification time, C_m is a constant specific to the material, V and A denote the volume and surface area of the casting, respectively. After the metal was cooled to normal temperature, the sand mold was broken apart to get the hardened steel casting. The surface roughness of the casted metal with and without the application of mold coating was measured with a surface roughness profilometer.

3. Results & Discussion:

3.1. Sieve Analysis:

Foundry coatings are typically made up of refractory aggregate, binder, sintering agent, suspending agent, solvent, additives, and other components [6]. Zircon

serves as the principal constituent/ refractory aggregate for foundry coatings with dextrin as the coating's binder. The chemical composition of zirconium sand used for foundry coating is tabulated in table 4.

Table 4: Zirconium Sand composition

Name of Substances	% Composition
Zirconia & Hafnia	64.2
Silica	33.8
Alumina	0.90
Titania	0.14
Iron Oxide	0.06

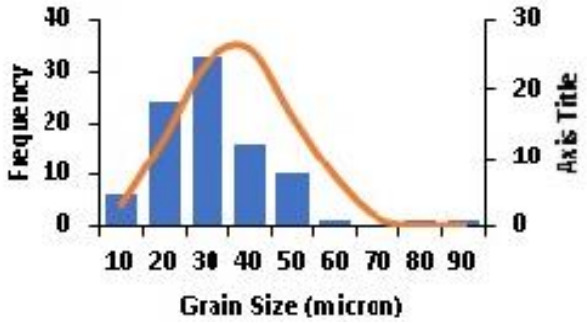

Figure 4. Histogram shows grain size

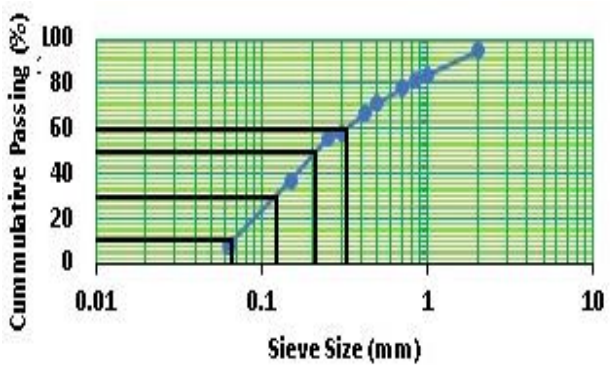

Figure 5: Comulative curve for percentile value

The average mesh number of silica molding Sand is nearly 64. The zircon powder has a mesh size from -200 to -325, a particle size distribution primarily between 35 and 45 microns, making it finely ground and suitable for specific applications that require a finer particle size range. Fig. 4 shows the particle size distribution curve. 10% of the particles (D10) are smaller than 65 microns and it is an effective size of particles, 30% of the particles (D30) are smaller than 130 microns and 60% of the particles (D60) are smaller than 330 microns. This distribution curve clearly shows that this sand sample has a good representation of all particle sizes. Hence this curve is said to be representing a well-graded sand. A coefficient of uniformity is used to classify the sand gradation and it is 4.94 for the silica sand which means that the grain size spans a large range and is an indication of well-graded sand. With the coefficient of uniformity equal to 1 means grains are all the same size and is poorly graded sand. The coefficient of curvature describes the general shape of the gradation curve. Despite the good distribution of the curve, the coefficient of curvature for the silica sand is 0.68. If the coefficient of curvature is between 1 and 3 then it is a smooth curve and is well-graded sand. If it is less than 1 or greater than 3 then the curve is not smooth and is poorly graded sand.

3.2 FTIR:

The FTIR spectrum of alcohol-based zircon coating is shown in fig. 6. The zircon coating contains zircon sand, dextrin as a binding agent, phenol formaldehyde resin and ethanol. The spectra show a range of peaks from different constituents of the coating. The band shown at 560 cm^{-1} is for Zr-O stretching vibrations in the ZrO_2 phase [13-16].

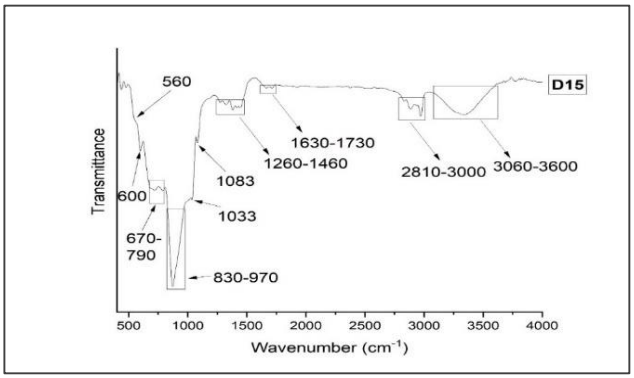

Figure 6: FTIR analysis of Alcohol-based zircon coating

The small peaks from zircon and dextrin overlap in the region from 670 cm^{-1} to 790 cm^{-1}. The details of the hidden bands in this region are as follows. The band at 716 cm^{-1} results from an asymmetry in the stretching of Zr-O-Zr [16]. The small band at 747 cm^{-1} and 750 cm^{-1} are also from Zr-O stretching vibrations [13-15]. The bands at 760 cm^{-1} shows the bending vibrations outside the plane of CH and the bands at 712, 709, 680, and 681 cm^{-1} correspond to the bending vibrations outside the plane of the hydroxide groups from dextrin [17].

The broad peak covers a range from 830 cm^{-1} to 970 cm^{-1}. Under this broad peak, many small peaks exist. The peaks at 856, and 853 cm^{-1} correspond to the

bending vibrations outside the plane of CH and the peak at 932 cm^{-1} is related to ring bond vibrations from dextrin [17]. The overlapped peak at 876 cm^{-1} shows Aromatic C-H wag in PF Resin [18]. The band at 1,028 cm^{-1} which is overlapped by broad peak of 830-970 cm^{-1},corresponds to the C–O–C stretching [19]. The ether bond between benzene rings at 1011.5 cm^{-1} is present in PF Resin [20]. The band at 1078 cm^{-1} is related to the stretching vibrations of the C-O bonds [17]. Also, the overlapped band at 1103 cm^{-1} is due to the vibration of the C-O bond in dextrin [21]. Aromatic C-H in-plane deformation at 1092 cm^{-1} is observed in PF Resin [18]. The C-O stretching at 1092 cm^{-1} can be observed in ethanol [22]. There are many small peaks within1260-1460 cm^{-1} this region. The small band at 1380 cm^{-1} suggests that the hydrated molecules may be present in hydroxyl groups in ethanol [16]. Moreover, the peak at 1369 cm^{-1} is related to the bending vibrations of the CH_3 and CH_2 groups in dextrin [17]. At 1327 cm^{-1} CH_3 deformation is observed. A methylene in PF resin shows an abending pattern at 1458 cm^{-1}. An Aliphatic CH_2 scissor bend is present at 1458 cm^{-1} [18]. The band at 1239.3 cm^{-1} was the C-O stretching vibration peak on phenol rings in PF Resin [20]. The peak at 1271 cm^{-1} is due to stretching vibrations of the C–O–C ether linkages in PF [23]. The C-O stretching at 1384 cm^{-1} is observed in ethanol [22]. The FTIR spectrum of ZrO_2 displays the peaks at 1633 cm^{-1} [14-16]. The peak at 1651 cm^{-1} is attributed to the alcohol molecule's bending vibration [17]. Peaks at 1639 cm^{-1}, and 1641 cm^{-1} are carboxyl group in dextrin [21]. In general, the individual bands for carbonyl stretching of carboxylic acids are observed at 1712 cm^{-1} [19]. At 1607 cm^{-1}, the C-C aromatic ring stretches in PF resin [18]. There were special C=C stretching vibration peaks of benzene ring skeletons at 1641.3 cm^{-1} in PF [20]. The absorption peaks at 1630 cm^{-1} are characteristic of formaldehyde and are due to the stretching vibrations of the C=C bonds in PF resin [23]. Moreover, the peak at 2937 cm^{-1} belonged to the CH bond's stretching vibrations of dextrin [17]. The bands due to CH stretching vibration were in the region of 2930 cm^{-1}, 2928 cm^{-1} and 2935 cm^{-1} in dextrin [21]. Another band at 2,927 cm^{-1} represents the vibration due to C–H stretching [19]. Methylene has two stretching modes at 2910 cm^{-1} and 2850 cm^{-1} in PF resin. Aliphatic CH_2 symmetric stretch is observed in PF resin [18]. **T**he C-H stretching at 2980 cm^{-1} can be seen in ethanol [22]. The O-H stretching vibrations band of adsorbed water molecules are reflected in the broad, sharp peaks at 3416 cm^{-1}. The appearance of this peak may be due to the chemisorption of water molecules readily on the ZrO_2 surface when exposed to atmosphere conditions [16]. A peak at 3339 cm^{-1} is related to the OH group's stretching vibrations in the dextrin molecules [17]. The band due to hydroxyl stretching vibration was observed in the region of 3400 cm^{-1}, 3434 cm^{-1} and 3424 cm^{-1} [21]. A band at 3386 cm^{-1} corresponding to the stretching vibration of O–H [19]. A broad peak at 3440 cm^{-1}, assigned to the stretching vibration of phenolic hydroxy at 3005 cm^{-1} shows C-H aromatic stretching, is found in PF resin [18]. The strong and wide absorption band at 3430.9 cm^{-1} was the stretching vibration absorption peak of the associated hydroxyls [20]. Regarding the spectrum of phenol–formaldehyde, a broad peak at 3343 cm^{-1}, which is due to the stretching vibrations of the -OH groups in phenol, can be seen [23]. The O-H stretching at 3366 cm^{-1} can be seen in ethanol [22].

3.3. Weight of Sample before and after ignition:

The sand mold-coated samples were flame ignited to evaporate the volatile materials

Figure 7: Flame ignition of alcohol-based zircon coating on sand mold

from the surface of the mold for 40 seconds as shown in fig. 7. The weight of the samples before and after ignition and the weight loss of each sample are tabulated in table 5.

Table 5: weight of coated samples before and after ignition

Weight (gm)	Sample-15	Sample-17	Sample-20
Initial	114	122.5	136.4
Final	109.2	117.5	131.1
Difference	4.8	5	5.3

It can be seen that with the increase in dextrin content, the weight loss increases. All three samples were then placed in an oven for weight loss at 140°C. This data serves as an indicator of any changes or reactions occurring during the experimental process to 140°C temperature at an interval of 10 minutes. The weight loss of the samples was subsequently measured and the graph in fig. 8 shows the % weight loss with time.

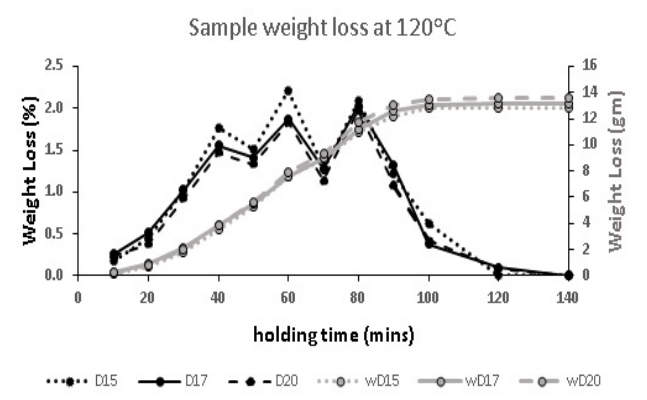

Figure 8: Weight loss vs time graph

It can be observed from the above fig. 9 that heating the samples to 120°C helped in evaporating the organic compounds from the sand mold. The % weight loss and weight loss in gram curves show that at 120°C there is no further weight loss. All the organic/volatile compounds have been evaporated/ decomposed.

The samples were then further heated to 200°C, 400°C, 600°C and 1200°C to observe the deterioration and delamination of the coating. Fig. 9 shows the behavior of coated samples heating at different temperatures.

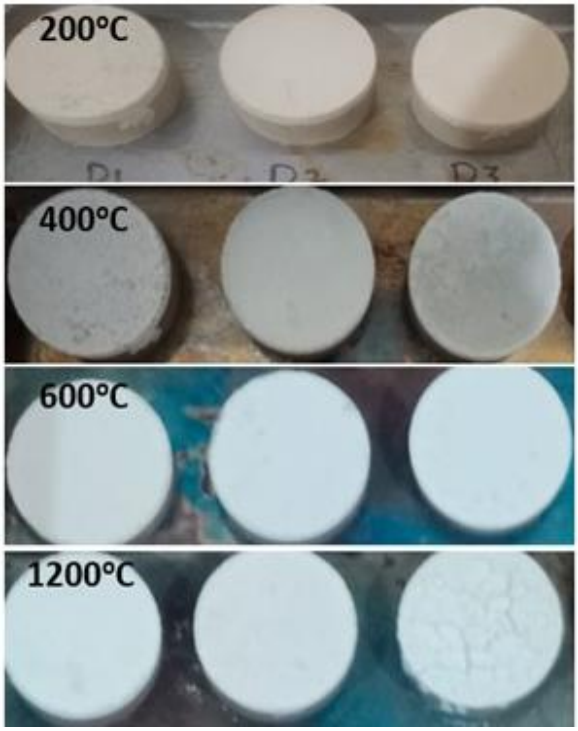

Figure 9: Samples heated at varied temps.

It is observed that at 200°C, 400°C and 600°C the coating is intact and no delamination and flakes are observed. Whereas, the samples heated at 1200°C with the highest dextrin content shows few surface cracks. Overall, no sign of chipping off of the coating is observed.

A sand mold must be strong enough to resist the molten metal pressure during pouring and have dimensional stability, gas permeability & good collapsibility after solidification. A binder plays a very important role in improving the mechanical properties of the mold. With increasing the dextrin content, the mechanical strength of the mold increases [24] but there is a tradeoff between mold-breaking and high gas evaluation during solidification [25].

3.4. Surface Roughness & Thickness:

Alpha set sand molds are coated with the developed coating by a spray gun. The average coating thickness achieved is measured to be 89 microns as shown in fig.10.

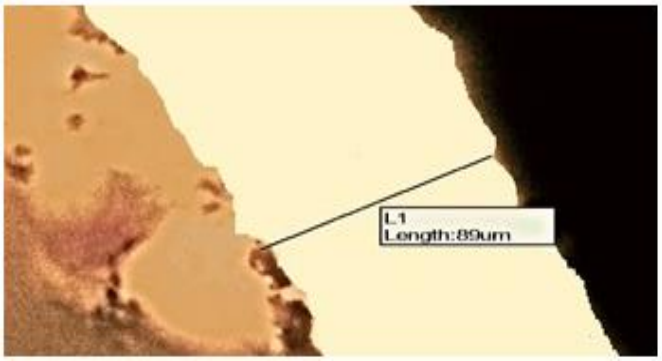

Figure 10: Cross section of Alcohol-based zircon coating thickness on silica sand mold.

The surface roughness of the three different coating compositions was the same because the change in dextrin amount in the coating composition did not make any principal change in surface roughness. The average surface roughness values of the silica sand mold with and without coating presented in table 6. The surface roughness of the sand mold sample without coating was 7 microns. With the application of coating, the average surface roughness of the silica sand mold decreases with increasing dextrin content. Coatings on the sand mold's surface made the surface smoother. The decrease in average surface roughness is consistent with an increase in dextrin content.

Table 6: Average Surface roughness (Ra) of sand mold with and without zircon coating

Without Coating (µm)	With coating (µm)		
D-N	D15	D17	D20
7.04±1.52	2.28±0.47	1.72±0.07	1.12±0.11

3.5. Permeability:

The permeability number of the coating samples is shown in table 7.

Table 7: Effect of variation of dextrin composition on permeability number

Table 7: Effect of variation of dextrin composition on permeability number

Without Coating (Permeability Number)	With coating (Permeability Number)		
D-N	D15	D17	D20
200	182	164	154

The permeability of sand mold during the casting process refers to the sand's ability to allow gases to pass through. This characteristic is crucial for preventing defects in the casting by allowing gases generated during the pouring and solidification processes to escape. High permeability ensures better-quality castings with fewer gas-related issues.

The grain size of the silica molding sand is around 130 microns. The function of the binder is to hold the sand collected and the permeability number of the silica sand mold is 200. By spraying an alcohol-based zircon coating with variation in dextrin content, onto the sand mold surface reduces the permeability of the molding sand from 9% to 23% than in the case of the sand without a coating. The decrease in permeability number is very much consistent with an increase in dextrin content. The zircon sand has an average particle size of 40 microns. When the zircon coating is applied to the sand mold, the zircon particles fill the gaps/pores on the surface of the mold. Since the silica sand has an average particle size of 130 microns and the surface roughness of the sand mold without coating is high, the zircon particles easily adjusted into the pores on the surface and because of the filling of the gap, the surface roughness of the sand mold with zircon coating reduces. The change in permeability of the molding sand is due to the grain size of zircon sand and the thickness of the coating [26]. The zircon sand particles penetrated the surface of the molding sand, filled the pores with appropriate particles and then built up the coating on top of the molding sand. Zircon sand has low thermal expansion but good thermal conductivity which is used to help solidification [27]. The zircon coating as a protective layer on the silica sand mold that helps to keep the dimensional stability of the mold because of the large nonlinear expansion of the silica sand during alpha to beta transition at around 573^{o}C [28], and this expansion of silica is worse in steel castings. Zircon coating acts as a protective coating and when it is applied, it improves the casting surface quality, by eliminating a range of surface defects. The thick protective coating on the mold lowers the permeability of the molding sand and this low permeability of the sand mold hinders the release of gas when the molten metal is poured. The trapped gas may cause misruns, external gas cavities, pitted skin, punctures and others.

After the completion of the casting, the average surface roughness of as-casted four samples were tested. The results obtained are provided in table 8.

The surface roughness results of the casted samples obtained from the coated molds show almost the same surface roughness value with a variation of dextrin content.

Table 8: Average Surface roughness (Ra) of as casted steel samples with and without zircon coating on sand mold

Without Coating (µm)	With coating (µm)		
D-N	D15	D17	D20
233±48.93	180±39.60	175±8.75	166±16.61

The casted sample obtained from the uncoated sand mold shows nearly 34% more surface roughness than the samples obtained from the coated mold. The increase in surface roughness is due to the porosity on the surface of the sand mold where whereas the zircon coating on the sand mold filled the gaps with zircon particles being smaller sand particles than zircon.

3.6. Interface Reactions:

During the liquid metal pouring into the sand mold, the molten metal penetrates the pores of the sand mold leaving the rough surface of coating. Some physical and chemical reactions take place at the metal-mold interface, including the reaction of alloying elements with the molding sand. The zircon coating application onto the sand mold and core prevents the metal-sand interface reactions. The degree of liquid metal penetration to the pores of the sand mold depends on the density of the metal to be cast. In the present case of steel casting, having high density, the penetration is severe at the bottom of the mold which leads to the high permeability of the molding sand and high surface roughness of the cast. Metal penetration and surface defects in the casting occur frequently in ferrous metal casts due to their high casting temperature, high density and high reactivity of alloying elements (oxides) to silica sand. The metal oxidation reaction given below takes place during the liquid metal pouring in the sand mold and even during solidification. For carbon steel, among the oxides, iron oxides prevail, primarily iron (II)-oxide (FeO) with a melting temperature of 1370 °C.

$$Fe_{(l)} + ½O_{2(g)} = 2FeO_{(l)}$$

$$\Delta G=529800-113.0T \quad (3)$$

The carbon as an alloying element in molten metal reacts with oxygen during liquid metal pouring to form carbon monoxide (CO) and further addition of oxygen converts CO to carbon dioxide (CO_2).

$$C_{(s)} + ½O_{2(g)} = CO_{(g)} \quad (4)$$

$$CO_{(g)} + ½\ O_{2(g)} = CO_{2(g)} \quad \Delta G=-394{,}000+0.0T \quad (5)$$

$$H_2O \text{ (moist sand)} = H_2 + ½O_2 \quad \Delta G=57{,}000-0.0T \quad (6)$$

Manganese as an alloying element also reacts with oxygen during the pouring process.

$$2Mn_{(s)} + O_{2(g)} = 2MnO_{(l)} \quad (7)$$

The thermodynamics of oxides (FeO, Fe_2O_3, MnO) and silicates (FeOMnO-SiO_2, MnO-SiO_2) produced during the solidification are discussed by many researchers [29].

The temperature during the pouring of liquid metal reaches 1550°C to1600°C. This high temperature causes dehydration, oxidation, and formation of other compounds like silicates[30]. The application of zircon coating in a sand mold having properties like a low coefficient of thermal expansion, not readily wetted by liquid metal and minimal gas production when in contact with liquid metal, make it suitable as a protective coating for the mold and core [31].

4. Conclusion:

Alcohol-based zircon sand coatings were prepared with varying dextrin content (D15, D17, D20) for steel castings. The zircon sand used for coating is well-graded with an average particle size of 40 microns. The FTIR results show the presence of Zr-O stretching (Zircon sand) and functional groups from dextrin and PF resin. The dextrin-varying composition did not make any significant difference in FTIR peaks. The three coating compositions were ignited to 120°C to evaporate the volatile materials and the initial weight loss of the coating in all three 3 compositions was 7.69±0.23 grams. The thermal stability of the coating was checked at 200°C, 400°C, 600°C and 1200°C. The coatings demonstrated stability up to 1200°C without delamination or cracking. Silica sand molds were prepared by the alpha set sand molding process. The sand molds were sprayed with three different coating

compositions. The average coating thickness on silica sand mold was 89 microns. An average surface roughness of the sand mold with coating was decreased by 3 folds as compared to the molds with no coating also the surface roughness decreases with increasing the dextrin content. Similarly, the average surface roughness of the steel casting obtained from the coated mold was 25% lower than that of the casting obtained from the uncoated mold. Again, the average surface roughness of the steel casting decreases with increasing the dextrin content. The permeability of the coating was reduced by 9%, 18% and 23% by increasing the dextrin content in the coating in comparison with the permeability of the sand mold, respectively, which prevented the casting defects caused by metal penetration. With the application of the coating, the mold-sand interface reactions were controlled by lowering the wetting of the coated sand mold with liquid metal and subsequent minimal gas production when in contact with liquid metal, making it suitable as a protective coating for the mold and core.

5. References:

[1] A. Kmita , J. Zych, M. Holtzer, J. Mocek, and S. Piasny, "Ecological water - based protective castings for moulds and cores of iron castings," *Metalurgija*, vol. 55, 2016.

[2] U. C. Nwaogu, and N. S. Tiedje, "Foundry Coating Technology: A Review," *MSA*, vol. 2, 2011, DOI :10.4236/msa.2011.28155.

[3] G. Milanova, "Foundry Coatings - Review," *J. Mater. Eng.,* vol. 1, no. 1, 2023, DOI: 10.61552/JME.2023.01.006.

[4] Q. Bian, S. Feng, H. Dong, and S. Xie et al., "Process Characteristics of Water-based Self-curing Coatings for Sand Casting," *J. Phys. Conf. Ser.*, vol. 2109, no. 6, 2021, DOI:10.1088/1742-6596/2109/1/012026.

[5] M. Wasim, A. Salam, K.M. Deen, and H. Rehman, "Development and characterization of foundry refractory coating and validation through factorial design of experiment," *JPIChE*, vol. 48, no. 1, 2022.

[6] C. Zhan, S. Feng, S. Xie, C. Liu, Y. Gao, and J. Liang, "Anti-carburizing Coating for Resin Sand Casting of Low Carbon Steel Based on Composite Silicate Powder Containing Zirconium," *MATEC Web COnferences*, vol. 142, 2018. doi.org/10.1051 /matecconf /2018 14203007.

[7] G. L. Muoio, and N. Tiedje, "Achieving Control of Coating Process in your Foundry," *Arch. Foundry Eng.*, vol. 15, no. 4, 2015, DOI: 10.1515/afe-2015-0089

[8] Z. L Xu, J. Wang, S. S. Yang, Q. L. He and H. Sh. Xiong, "Application of alcohol based spraying coating on green sand mould for steel casting," *IOP Conference Series: Materials Science and Engineering*, vol. 103, no. 1, 2015, DOI:10.1088/1757-899X/103/1/012012.

[9] Ł. Jamrozowicz, J. Zych, and J. Kolczyk, "The drying kinetics of protective coatings used on sand molds," *Metalurgija*, vol. 54, 2015.

[10] I. O. Leushin, and A.N. Grachev, "Anti-penetration coatings for foundry molds and cores based on slag of secondary aluminum metallurgy," *CIS Iron and Steel Review*, vol. 4, 2002.

[11] American Foundry Society Mold & Core Test Handbook, American Foundry Society, ed. 20205th.

[12] D. Anand, G. Aishwarya, D. Pratik, P. Pratik, V. Tejashree, and C. Ganesh, "Study of mould hardness for alpha set type resin bonded moulding sand system using Taguchi approach for metal casting applications," *MATEC Web of Conferences*, vol. 144, 2018, DOI.org/10.1051 /matecconf /201814403007

[13] S. Sagadevan, J. Podder, and I. Das, "Hydrothermal synthesis of zirconium oxide nanoparticles and its characterization," J. Mater. Sci.: Mater. Electron., vol. 27, no. 6, 2016, DOI 10.1007/s10854-016-4469-6.

[14] S. Kataria, M. K. Rain, A. Kumar, and H. Mudila, "Preparation and exploration of optical performance of novel polythiophene-ZrO2 composites," *Opt. Quantum Electron.,* vol. 56, no. 3, 2023, https://doi.org/10.1007/s11082-023-06046-3.

[15] S. Wang, S. Zhou, J. Huang, G. Zhao, and Y. Liu, "Attaching ZrO_2 nanoparticles onto the surface of graphene oxide via electrostatic self-assembly for enhanced mechanical and tribological performance of phenolic resin composites," *J. Mater. Sci.*, vol. 54, no. 11, 2019, https://doi.org/10.1007/s10853-019-03512-w.

[16] H. Basavanagoudra, "Designing a novel, ultra-sensitive, and biocompatible electrochemical nano-biosensor for the detection of tryptophan and bovine serum albumin using zirconium dioxide nanostructures," *Chem. Phys. Impact*, vol. 8, 2024, https://doi.org/10.1016/j.chphi.2024.100516

[17] A. Tohry, R. Dehghan, P. Hatefi, and S. C. Chelgani," A comparative study between the adsorption mechanisms of sodium co-silicate and conventional depressants for the reverse anionic hematite flotation," *Sep. Sci. Technol.*, vol. 57, 2021, https://doi.org/ 10.1080/ 01496395. 2021. 188 7893.

[18] H. Jiang, "The pyrolysis mechanism of phenol formaldehyde resin,"*. Polym. Degrad. Stab*., vol 97, 2012, DOI:10.1016/ j.polymdegradstab. 2012. 04. 016.

[19] S. Pradhan, S. Mohanty, and S. K. Nayak, "Waterborne epoxy adhesive derived from epoxidized soybean oil and dextrin: Synthesis and characterization," *Int. J. Polym. Anal. Charact*., vol. 22, no. 4, 2017, http://dx.doi.org/ 10.1080/ 1023666 X.2017.1295516

[20] Z. Wu, "Plasma Treatment Induced Chemical Changes of Alkali Lignin to Enhance the Performances of Lignin-Phenol-Formaldehyde Resin Adhesive," *J. Renew. Mater.*, vol. 9, no. 11 2021, DOI: 10.32604/jrm.2021.016786.

[21] R. Z. Ahmed, K. Siddiqui, M. Arman, and N. Ahmed, "Characterization of high molecular weight dextran produced by Weissella cibaria CMGDEX3," *Carbohydr. Polym*., vol. 90, no. 1, 2012, http://dx.doi.org/10.1016/ j.carbpol. 2012. 05. 063.

[22] S. K. A. Mudalip, M. R. Abu Bakar, F. Adam, and P. Jamal, "Structures and Hydrogen Bonding Recognition of Mefenamic Acid Form I Crystals in Mefenamic Acid/Ethanol Solution,"*. IJCEA*, vol. 42013, DOI:10.7763/IJCEA.2013.V4.277.

[23] E. Papadopoulou, I. Chrysafi, K. Karidi, A. Mitani, and D. N. Bikiaris, "Particleboards with Recycled Material from Hemp-Based Panels," *Materials,* vol. 17, no. 139, 2024, https://doi.org /10.3390 /ma17010139

[24] S. Mitra, A. R. de Castro, and M. El Mansori, "On the rapid manufacturing process of functional 3D printed sand molds," *J. Manuf. Process.*, vol. 42, 2019, https://doi.org/10.1016/j.jmapro.2019.04.034.

[25] D. Snelling, C. Williams, and A. Druschitz, "A Comparison of Binder Burnout and Mechanical Characteristics of Printed and Chemically Bonded Sand Molds," *International Solid Free form Fabrication Symposium*, University of Texas at Austin, USA, 2014, http://dx.doi.org /10.26153/ tsw / 15677

[26] Ł. Jamrozowicz, and A. Siatko, "The Assessment of the Permeability of Selected Protective Coatings Used for Sand Moulds and Cores," *Arch. Foundry Eng.,* vol. 20, no. 1, 2020.

[27] F. Peters, R. Voigt, S. Z. Ou, and C. Beckermann, "Effect of mould expansion on pattern allowances in sand casting of steel," *Int. J. Cast Met. Res.*, vol. 20, no. 5, 2007, https://doi.org /10.1179/ 136404607 X 268247.

[28] Z. Janjušević, Z. Gulišija, M. Mihailović, and A. Patarić, "Processes at the Inetrface Molten Metal-Sand Mold," *Metalurgija,* vol. 53, no. 2, 2014.

[29] Z. Janjusevic, "Chemical Thermodynamic Processes at Metal-Mold Interface," *Mater. Trans.,*vol. 54**,** no. 10, 2013, doi:10.2320/ matertrans. M2013190.

[30] L. Andrić et al., "Zircon-based coating for the applications in on foam casting process," *CI&CEQ*, vol. 18, no. 4, 2012, DOI 10.2298/CICEQ111122034P.